Borole/Thiophene Cooligomers and Copolymers with Quinoid Structures and Biradical Characters

Hui Cao, Jing Ma,* Guiling Zhang, and Yuansheng Jiang

Department of Chemistry, Institute of Theoretical and Computational Chemistry, Key Laboratory of Mesoscopic Chemistry of MOE, Nanjing University, Nanjing, 210093, P. R. China

Received July 17, 2004; Revised Manuscript Received November 15, 2004

ABSTRACT: The geometrical structures and electronic properties of borole/thiophene cooligomers are studied employing the density functional theory with B3LYP functional. The borole-containing oligomers have been suggested to have the quinoid structure and distinct biradical character. The introduction of thiophene rings into the oligoborole will retard the appearance of the quinoid structure and consequently stabilize the borole-containing oligomers. Electronic structrues of polyborole and borole/thiophene copolymers are investigated by the periodic boundary condition (PBC) and the cyclic oligomer model. Both the PBC and cyclic models predict the quinoid structure of borole/thiophene copolymer. The PBC calculations give estimations of band gaps of around 2.21 eV for the polyborole and 2.22 eV for the borole/thiophene (1:1) copolymer, which are different from those (∼0.00 eV) obtained by the oligomer extrapolation schemes.

1. Introduction

There is much interest and intensive research has been taking place in plastic electronics based on conjugated polymers with the perspective of obtaining various functional materials.[1,2] The exploration of the novel conjugated conducting polymer with small band gap, E_g, toward the dream of obtaining the truly synthetic metal[3] has always been an aim for striving and still remains to be a challenge to chemists. Another important consideration in the design of organic materials should be chemical stabilities of polymers. That is the reason polythiophene (**PT**), which is relatively more stable than polypyrole (**PPy**) and polyfuran (**PFu**), has aroused extensive interest both experimentally and theoretically.[4−6]

Recently, the boron-containing conjugated organic polymers have attracted much attention due to their intriguing electronic properties.[7−9] Since organoboron polymers can be viewed as homologues of electron acceptors through the vacant p-orbital of the boron atom, they are expected to become a new class of n-type conjugated polymers with unique characteristics. The pentaphenylborole, a derivative of borole, has been synthesized,[10] however, polyborole (**PB**), has not been reported yet. Salzner et al.[11] have theoretically demonstrated that the band gap of polyborole may vanish through an extrapolation scheme from oligomers, **1,** as shown in Figure 1a**,** to the polymer limit. The strong anti-aromatic nature of borole molecule has been shown by the large negative value of "resonance stabilization energy", or called "aromatic stabilization energy" (−0.98 and −0.97 eV obtained at the MP2(fc)/6-311+G(d,p)[12a] and BLYP/6-311G(d,p)//BLYP/6-31G(d)[12b] levels, respectively), in contrast with the large positive values for thiophene (0.81 eV[12]) and furan (0.64[12a] and 0.67 eV,[12b] respectively). This may cause the quinoid structure and instability of polyborole. The introduction of thiophene rings into the polyborole is intuitively anticipated to achieve a polymer with a narrow band gap and relatively higher stability. Thus, it is our purpose to theoretically study the electronic structures of borole/thiophene cooligomers, **2** and **3** (shown in Figure 1a), and copolymers, **4** and **5** (shown in Figure 1b), to provide useful information for understanding some interesting properties of borole-containing polymers and designing new experiments.

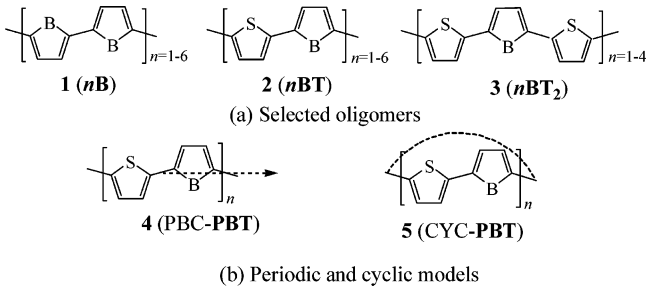

Figure 1. Structures of the studied systems. (The arrow in **4** represents the translation vector.)

Theoretically, the energy difference between the highest occupied molecular orbital (HOMO) and the lowest unoccupied molecular orbital (LUMO), which is referred to as the HOMO−LUMO gap, is usually considered as the first estimate of the band gap.[11,13] It is assumed that what underlies this approximation is that the lowest singlet excited state can be described by only one singly excited configuration in which an electron is promoted from the HOMO to LUMO. However, such a small band gap of polyborole (PB) extrapolated from HOMO−LUMO gaps of oligomers[11] implies that the borole ring may introduce the biradical character into borole-containing oligomers, **1**−**3**, for which the unrestricted theoretical methods are required to obtain reasonable results. Unfortunately, within the spin unrestricted framework, the transition between the singly occupied molecular orbital (SOMO) to its corresponding LUMO is seldom discussed because of the complexity caused by the fact that α and β spin orbitals often have different energies.

On the other hand, another practical method for estimating the band gap of a polymer may be the time-dependent density functional theory (TDDFT)[14,15] treatment by which transition energies from ground states to the first dipole-allowed excited states of oligomers are successively calculated and extrapolated to the limit of

10.1021/ma048534y CCC: $30.25
Published on Web 01/20/2005

a polymer.[16−19] Sometimes, however, applications of TDDFT may suffer from the systematical underestimation of excitation energies by 0.4−0.7 eV compared to experimental results.[16,20,21] The deviations in excitation energies of oligomers from experiments are probably caused by the fact that (1) there is a limitation of the current approximate exchange-correlation potential in the asymptotic region[22,23] and (2) theoretical predictions are made for the isolated gas-phase chains, while experimental band gaps are usually measured in the condensed phase.[6a] Therefore, it is desirable to directly compute the band gap of a polymer to eliminate the boundary effects of models for oligomer extrapolations. Usually, two models, the periodic (**4**) and cyclic (**5**) ones, are adopted in the simulation of a polymer. It is interesting to compare the performance of these two polymer models and to find out whether the DFT calculations with periodic boundary condition (PBC) can be applied to provide reasonable descriptions for polymers.

In this work, we will use the DFT method to study the electronic properties of borole/thiophene cooligomers,**1**−**3**, and use DFT with periodic boundary condition (PBC) to calculate the band gap of the borole/thiophene copolymer, **4**. The cyclic oligomers, **5** (n = 2−5), are also studied with the extrapolated band gap compared with the PBC calculation on **4**. We aim to understand factors affecting the relative stabilities and band gaps of borole-containing polymers by (1) investigating the biradical characters of the borole/thiophene cooligomers and elucidating the electronic structures of them and (2) calculating band gaps of polymers by the periodic boundary condition method and the extrapolation method.

2. Computational Details

The DFT and PBC calculations have been performed with Gaussian03 program.[24] Geometries and electronic properties are calculated by means of hybrid density functional B3LYP with the basis set of 6-31G*.

Unrestricted Descriptions of Biradical Characters. Both the spin-restricted and the spin-unrestricted broken-symmetry DFT method are employed to optimize geometries and to obtain the corresponding electronic structures, since most of the studied oligomers, **1**−**3**, have obvious biradical characters. It is well-known that when a molecule has the radical character the spin-unrestricted method with the broken-symmetry solution, in which the HOMO and LUMO orbital are mixed to destroy the $\alpha-\beta$ symmetry in the initial guess of the molecular orbital, can get lower ground-state energy than the spin-restricted method.[25−27]

Validations of PBC Calculations. The periodic boundary condition (PBC) is also employed to predict band gaps of polymers. The PBC/B3LYP calculation[28,29] has been recently implemented in the Gaussian03 program.[24] To validate the PBC calculations, we have carried out the PBC calculations on the *trans*-polyacetylene (***t*-PA**), polypyrole (**PPy**), poly(*p*-phenylene) (**PPP**), polythiophene (**PT**), and polyfuran (**PFu**) systems and compared PBC/B3LYP results with the previous TDDFT results by extrapolations,[16] other PBC calculations with the Perdew−Wang exchange-correlation functional[30] and plane wave basis set,[31] and experimental data (cf. Table 1).[32−38] In Table 1, we can see that band gaps of ***t*-PA** and **PPP** obtained from the PBC calculations still have some deviations from the experimental data, while the present PBC (with B3LYP functional) results of **PPy**, **PT**, and **PFu** polymers with the conjugated five-membered rings are in good agreement with experimental band gaps. The differences between them are no more than 0.1 eV. However, one cannot be too optimistic about such small deviations of PBC/B3LYP results from experimental data, since the interaction between the polymer chains and the possible defects on the backbone of chains are ignored here. The high accuracy of PBC/B3LYP band gaps for the studied polymers may benefit from the cancellation of errors. In the present work, we will investigate the applicability of the PBC/B3LYP scheme to calculate band gaps of borole-containing polymers with distinct biradical characters.

Table 1. Band Gaps, E_g (in Units of eV) Obtained by PBC and TDDFT Calculations,Where the Experimental Data Are Also Given for Comparison

	E_g				
polymer	PBC/B3LYP	PBC/PW[a]	PBC/VASP[b]	TDDFT[c]	exptl
***t*-PA**	1.16[d]		0.21	1.32	1.4[e]
PPP	3.06		1.86	2.97	3.02[f],2.8[g]
PPy	2.88	1.80	1.70	1.95	2.85[h]
PT	2.05	1.10	1.04	1.52	2.0[i]
PFu	2.42	1.34		1.69	2.35[j]

[a] Reference 30 with Perdew−Wang (PW) exchange-correlation functional by Dmol3. [b] Reference 31 by Vienna ab initio simulation package (VASP). [c] Reference 16. [d] The super cell, containing four carbon atoms, is adopted. [e] Reference 32. [f] Reference 33. [g] Reference 34. [h] Reference 35. [i] References 36 and 37. [j] Reference 38

Table 2. Energies (in Units of au) of Oligomers 1−3, E_{RB3LYP}, Obtained by the Restricted Method, E_S and E_T of Singlet and Triplet States Obtained by the Unrestricted DFT Method at the Level of 6-31G(d)

		unrestricted method	
oligomer	E_{RB3LYP}	E_S ($\langle S^2\rangle$)[a]	E_T ($\langle S^2\rangle$)[a]
***n*B** (**1**)			
$n=1$	−359.2598	−359.2638 (0.91)	−359.2600 (2.03)
$n=2$	−717.3479	−717.3805 (1.06)	−717.3804 (2.06)
$n=3$	−1075.4573	−1075.4990 (1.06)	−1075.4990 (2.06)
$n=4$	−1433.5745	−1433.6176 (1.06)	−1433.6176 (2.06)
$n=5$	−1791.6926	−1791.7362 (1.06)	−1791.7362 (2.06)
$n=6$	−2149.8109	−2149.8548 (1.06)	−2149.8548 (2.06)
***n*BT** (**2**)			
$n=1$	−732.0399	−732.0399 (0)	−732.0232 (2.02)
$n=2$	−1462.9019	−1462.9091 (1.09)	−1462.9082 (2.06)
$n=3$	−2193.7654	−2193.7872 (1.10)	−2193.7872 (2.10)
$n=4$	−2924.6315	−2924.6657 (1.10)	−2924.6657 (2.10)
$n=5$	−3655.5087	−3655.5442 (1.10)	−3655.5442 (2.10)
$n=6$	−4386.3869	−4386.4228 (1.10)	−4386.4228 (2.10)
***n*BT$_2$** (**3**)			
$n=1$	−1283.8607	−1283.8608 (0.24)	−1283.8544 (2.03)
$n=2$	−2566.5386	−2566.5447 (1.29)	−2566.5438 (2.05)
$n=3$	−3849.2170	−3849.2312 (1.38)	−3849.2311 (2.28)
$n=4$	−5131.8953	−5131.9177 (1.36)	−5131.9177 (2.33)

[a] The expectation values of S^2, $\langle S^2\rangle$, for the singlet (triplet) states reflect the extent of spin contaminations.

3. Results and Discussion

3.1. Oligomers. Energies of oligomers **1**−**3** calculated by both the spin-restricted and unrestricted DFT/B3LYP methods are listed in Table 2. To make this table more concise, we just show results of ***n*B** (**1**) with the integer number of n, while energies of **1** when n = $^1/_2$, $^3/_2$, ..., $^9/_2$, are given in Table S1 of the Supporting Information. It is interesting to find that when oligomers are larger than the borole (**1**, n = $^1/_2$) and borole/thiophene cooligomer (**2**, n = 1), the spin-unrestricted calculations give lower energies of singlet states, E_S, than those obtained by the restricted DFT calculations, E_{RB3LYP}, suggesting that the radical character exists in the longer oligomers. For example, the total energy of **5BT** (**2**) is −3655.5087 au calculated by the spin-restricted method, in contrast, the spin-unrestricted method gives a value of −3655.5442 au, which is 0.966 eV lower than that calculated by the spin-restricted method. Therefore, the spin-unrestricted

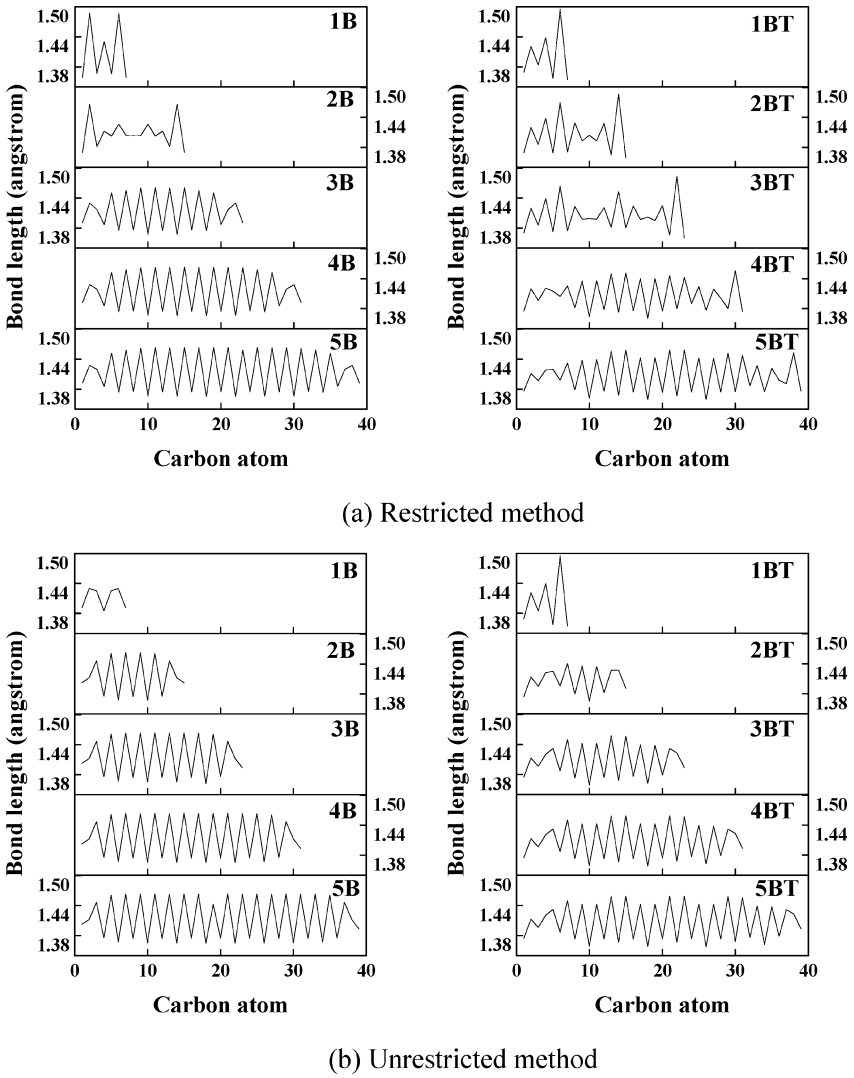

Figure 2. Carbon−carbon bond lengths varied with the number of C atom along backbones of oligomers, ***n*B** (**1**), and ***n*BT** (**2**) ($n = 1-5$), which are obtained by (a) the restricted and (b) the unrestricted methods, respectively.

method will give a better description on the electronic structure than the spin-restricted method.

Geometry. Since extents of the electron delocalization and π-conjugation are reflected by the behavior of bond-length alternation along the backbone of π-conjugated oligomers, we investigate the variance in bond lengths of oilgomers ***n*B** (**1**) and ***n*BT** (**2**) to find out the influences caused by the introduction of thiophene unit into borole oligomers. The behaviors of bond-length alternation calculated by both the spin-restricted and unrestricted DFT methods are depicted in Figures 2 and 3. From Figure 2a we find that for **3B** and **4BT** as well as for their longer homologues there exist some geometrical defects in the terminal parts of backbones as reflected by a jump of phase in the curve of bond-length alternation. Those defects are usually termed as the soliton regions, which are indeed radicals with the unpaired electrons.[39] Thus, the longer borole-containing oligomers have remarkable biradical nature, which will be discussed in the next subsection.

On the other hand, in comparison with ***n*B** (**1**), the introduction of thiophene rings in ***n*BT** (**2**) slightly retards the appearance of geometrical defects at terminal ends of backbones as shown by the transitional behavior (Figures 2a and 3a) between the aromatic and quinoid structures ($n = 2$ and 3). And from the spin-unrestricted method shown in Figures 2b and 3b, we can see that **1B** has already shown the biradical nature, whereas **1BT** remains to be aromatic form. Hence, both the spin restricted and unrestricted calculations reflect that the relative stability of polyborole is somewhat enhanced by the introduction of the thiophene unit.

Biradical Character. As mentioned above, the biradical character can be observed from the lower energies predicted by the broken-symmetry unrestricted method than those by the restricted methods (Table 2) as well as the bond length alternation behavior of ***n*B** (**1**) and ***n*BT** (**2**) (Figures 2 and 3). It can also be reflected by distributions of spin densities as shown in Figure 4, parts a and b. The spin density waves are gradually partitioned into two isolated parts when the degree of polymerization, *n,* of ***n*BT** increases. The local spin density wave reflects the distinct biradical nature; i.e., two radical centers come to be completely separated in the spatial region. Therefore, as long as there is the enough spatial extension in ***n*BT** cooligomers (**2**), the radical nature occurs.

The biradical nature in the borole/thiophene systems may be ascribed to the strong antiaromatic nature of the borole ring. As already mentioned in Introduction, the resonance stabilization energy of the borole molecule is calculated to be of a large negative value, −0.98 eV,

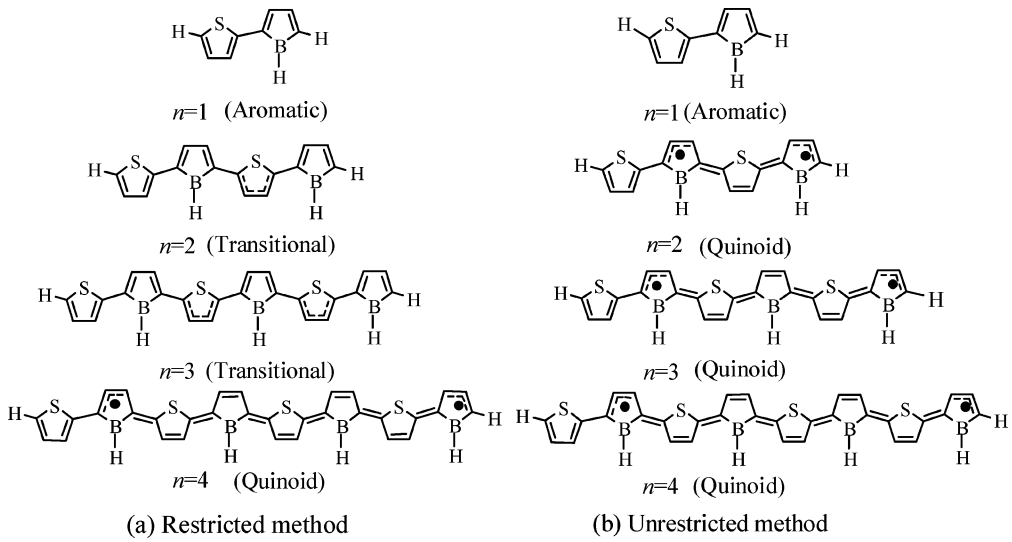

Figure 3. Evolvement of geometries of ***n*BT** (**2**) from the aromatic to quinoid structures with the increase of degree of polymerization calculated by the (a) spin-restricted and (b) unrestricted methods.

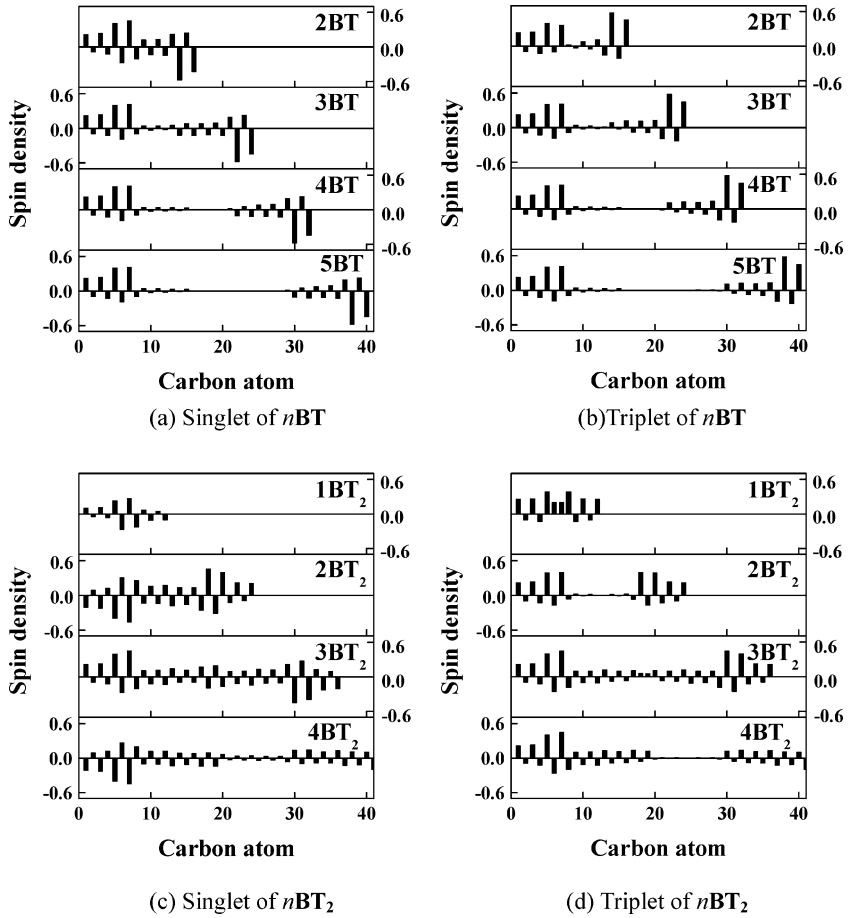

Figure 4. Distributions of spin densities of (a) singlet and (b) triplet states along the chain of ***n*BT** (**2**) as well as those (c) singlet and (d) triplet of ***n*BT$_2$** (**3**) (UB3LYP/6-31G(d)).

which is in contrast with the large positive value of 0.81 eV for the thiophene molecule (MP2(fc)/6-311+G(d,p)).[12] A natural idea of weakening the antiaromatic nature in the borole/thiophene cooligomer may be to increase the content of aromatic thiophene units. So, we design the ***n*BT$_2$** oligomers (**3**) to see if this ratio of borole to thiophene units can significantly eliminate the radical nature in the oligomer chain. The results in Table 2 and Figure 4, parts c and d, show that the biradical nature still exists in ***n*BT$_2$** (**3**) but is slightly diminished. In other words, stabilities of borole/thiophene cooligomers can be increased gradually with the increase in the content of thiophene units.

Since the borole-containing polymers have been found to have the distinct biradical character, an interesting question arises: whether the biradical polymer systems can exist stably? It is well-known that there is the electron spin resonance (ESR) signal in the neutral polyacetylene,[40,41]showing the existence of radical. But why radicals in polymers can stably exist while they are

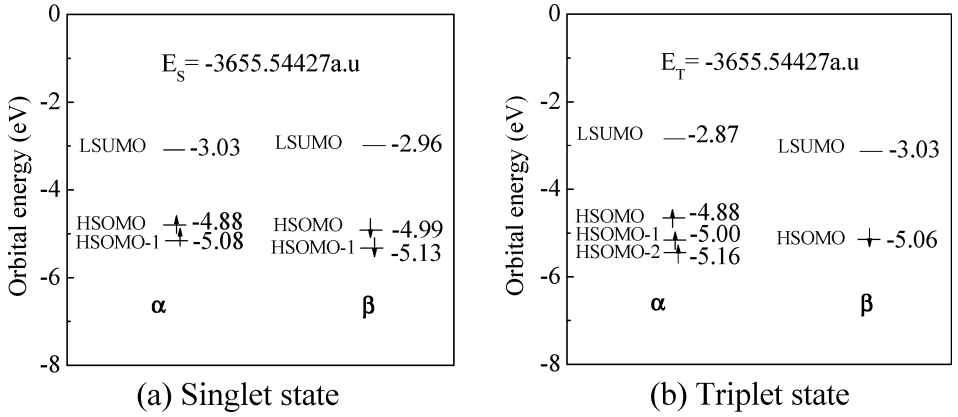

Figure 5. Total energy and energy levels of (a) singlet and (b) triplet states of **5BT** (**2**) obtained by the unrestricted method.

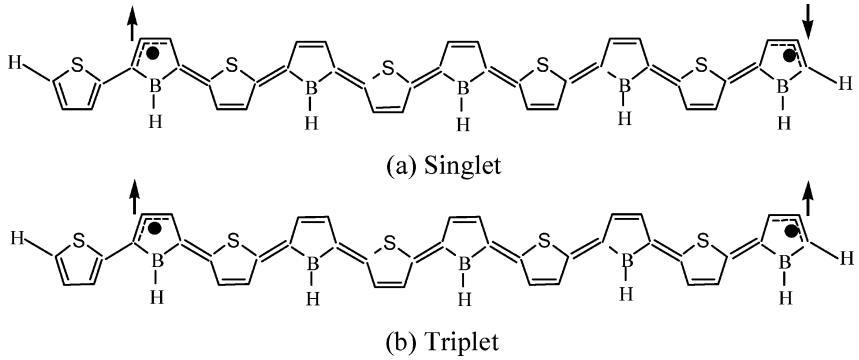

Figure 6. Schematic presentation of radical centers in (a) singlet and (b) triplet states.

very active and difficult to be located in small molecular systems? The radical electrons in polymers can give rise to the distortion of the ambient crystal lattices. This distortion of crystal lattices will in turn generate a strong potential well that causes the radical electrons to be localized. For **PB** and its copolymers (such as **PBT**), although they have not been synthesized yet, the simple analysis given above indicates the possibility of existence of such borole-containing systems.

Energy Levels and Energy Gaps. The HOMO−LUMO gap, Δ_{H-L}, obtained by the spin restricted method reflects the energy needed to destroy the chemical bond and form the unpaired electrons in an oligomer. This is corresponding to the ordinary energy band transition for a polymer. However, for biradical systems, the energy levels and gaps obtained by the unrestricted method become too complicate to have the direct significance of the band transition energy as addressed below.

In Figure 5, we take **5BT** as an example to show energy levels of spin orbitals. Since the unrestricted method is employed to the ***n*BT** oligomers with strong biradical characters, we should discuss energy levels of the singly occupied molecular orbitals (SOMOs) for α and β spin orbitals, respectively. The energy gap between the highest singly occupied molecular orbital (HSOMO) and the lowest singly unoccupied molecular orbital (LSUMO) is denoted by the HSOMO−LSUMO gap, Δ_{HS-LS}, for short. Energy levels of some spin orbitals of singlet and triplet states obtained by the unrestricted method are depicted in Figure 5, parts a and b, respectively. One can find that the singlet and triplet states of **5BT** are nearly degenerate in energy, which is also exhibited by the large spin contamination ($\langle S^2 \rangle = 1.10$) of the broken symmetry solution for the singlet **5BT** (cf. Table 2). In combination with the distribution of spin densities (Figure 4), we give schematic presentations of singlet and triplet biradicals of **5BT** in Figure 6, parts a and b, respectively.

The HOMO−LUMO gaps (Δ_{H-L}) and the gaps between the HSOMO and LSUMO of α or β spins (Δ_{HS-LS}) for oligomers **1**−**3** obtained by the restricted and unrestricted methods, respectively, also show us some interesting trends (with the detailed data listed in Table S2 of the Supporting Information). Figure 7 presents the different trends between the Δ_{H-L} and Δ_{HS-LS} (in singlet states from α to α orbital) as increasing the thiophene contents in cooligomers from **1** to **3**. The results of oligomers **1**−**3** with the identical numbers of rings, 6 and 12, are selected to make the comparison of energy levels and gaps (Figure 7). The trend of **1** > **2** > **3** in Δ_{HS-LS} gaps of ***n*B** (**1**), ***n*BT** (**2**), and ***n*BT$_2$** (**3**) varied with the increase in the content of thiophene units is opposite to that of **1** < **2** < **3** in their HOMO−LUMO gaps (Δ_{H-L}). From the HOMO−LUMO gaps, one can find that the introduction of thiophene units into the ***n*B** backbone does enlarge the Δ_{H-L}, implying the stabilization effect caused by thiophene rings. This is in coincident with the above-mentioned postponement of the appearance of quinoid structures in borole-containing oligomers by thiophene units (Figure 3). On the other hand, with the increase in the thiophene content, the HSOMO gradually shifts to higher level and the LSUMO drops to lower energy; consequently, the HSOMO−LSUMO gap (Δ_{HS-LS}) decreases in the order ***n*B** (**1**) > ***n*BT** (**2**) > ***n*BT$_2$** (**3**). Similar to the Peierls effect,[42] the elimination of the nearly degenerate spin orbitals may be corresponding to the enlargement of the HOMO−LUMO gap to gain the stabilization effect. Further studies toward the understanding of this phenomenon are still underway in our laboratory.

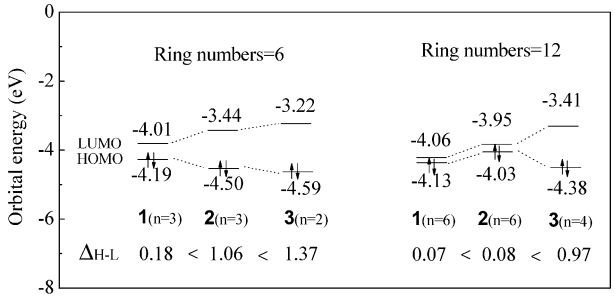

(a) HOMO-LUMO gaps

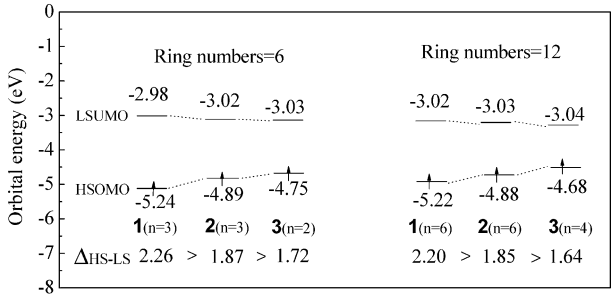

(b) HSOMO-LSUMO gaps

Figure 7. (a) HOMO−LUMO gaps (Δ_{H-L}) and (b) HSOMO−LSUMO gaps (Δ_{HS-LS}) of ***n*B** (**1**), ***n*BT** (**2**), and ***n*BT$_2$** (**3**) varied with the increase in the content of thiophene units.

Table 3. Band Gaps, E_g, Obtained by PBC Calculations on PB (1) and PBT (4), and the Extrapolation of HOMO−LUMO Gaps (Δ_{H-L}) from the Cyclic *n*BT Oligomers 5 and Acyclic Oligomers 1 and 2 to a Polymer Limit (in units of eV)

models	Δ_{H-L}	E_g
polyborole (**PB**)		
***n*B** (**1**, $n\rightarrow\infty$)		~0.00
PBC−**PB**		2.21
borole/thiophene copolymer (**PBT**)		
***n*BT** (**2**, $n\rightarrow\infty$)		~0.00
PBC−**PBT** (**4**)		2.22
CYC−***n*BT** (**5**)		
$n = 2$	3.11	
$n = 3$	2.63	
$n = 4$	2.35	
$n = 5$	2.28	
$n\rightarrow\infty$		2.00

3.2. Band Gaps of Polymers. The Periodic Boundary Condition Calculations. As we mentioned in section 2, the PBC band gaps of polymers constructed with five-membered rings, such as **PT**, **PPy**, and **PFu**, are in better agreement with the experimental data than those obtained by oligomer extrapolation scheme (cf. Table 1). However, the borole-containing oligomers have been predicted to have remarkable biradical characters with the radical centers localized at both ends of chains. It is expected that the PBC calculations with the translational invariance on such borole-containing polymers might mask biradical characters in backbones and may give a different description of the band gap from that extrapolated from properties of oligomers. The PBC calculations on **PB** and **PBT** do give us a larger band gaps than those estimated by oligomer extrapolations (Table 3). For example, the band gap of **PB** was extrapolated to be of zero from the Δ_{H-L} of ***n*B** (**1**) oligomers by Salzner et al.[11] as well as our present work, but the PBC/B3LYP computation yields a band gap of 2.21 eV. Even though, the PBC calculations obtain the similar ground-state geometry as the optimized structures of long oligomers. Taking **PBT** as an example, Table 4 lists structures of the polymer models, from which the quinoid geometry in the PBC cell is observed. Such a quinoid structure with PBC is almost identical to that in the **5BT** (cf. Table 4).

Table 4. Optimized Geometry of *n*BT (2, $n = 5$), PBC−PBT (4), and CYC−PBT (5, $n = 5$) Models

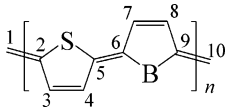

models	R_{1-2}	R_{2-3}	R_{3-4}	R_{4-5}	R_{5-6}	R_{6-7}	R_{7-8}	R_{8-9}
***n*BT** (**2**, $n = 5$)[a]	1.374	1.443	1.359	1.443	1.373	1.458	1.367	1.458
PBC−**PBT** (**4**)	1.375	1.443	1.360	1.443	1.374	1.459	1.365	1.459
CYC−**PBT** (**5**)	1.373	1.446	1.357	1.446	1.373	1.463	1.364	1.463

[a] The geometry of the central unit is adopted here.

The Cyclic Model. In addition to the PBC/B3LYP calculations, the cyclic polymer models can also eliminate the so-called "end effect" and hence be viewed as a system with periodic condition. It is interesting to compare performances of these two periodic polymer models, **4** and **5**.

First, the extrapolated band gap of CYC−**PBT** (**5**) from HOMO−LUMO differences is 2.00 eV (using the classical empirical "1/n" extrapolation method[11,30]), which is slightly smaller than the PBC band gap (2.22 eV). This deviation may be ascribed to strain in the bending backbones in the cyclic oligomers, especially in those small cycles. Figure 8 depicts the bending structure of cyclic borole/thiophene cooligomer **4BT** (**5**, $n = 4$). It is

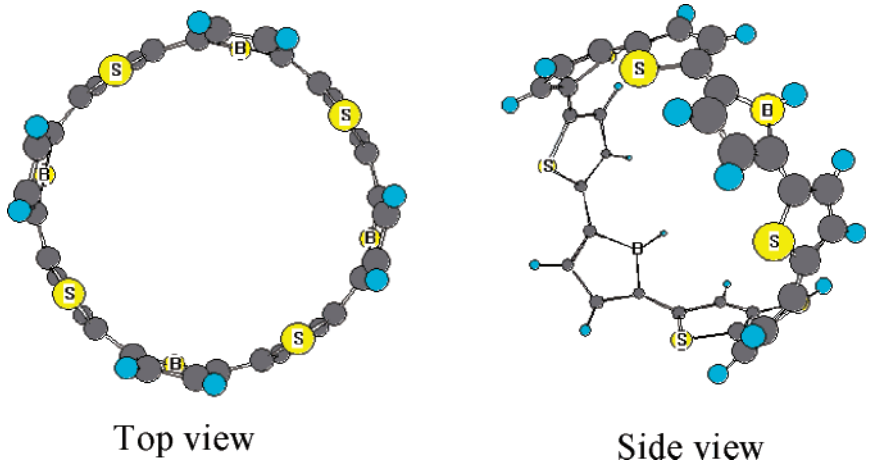

Figure 8. Optimized geometry of the cyclic borole/thiophene cooligomer **4BT** (**5**, $n = 4$).

well recognized that the coplanarity in oligomer backbones is essential for achieving the efficient delocalization of π electrons. However, for the small cyclic systems, backbones are far from the coplanarity. Only when the system with more and more units, can this requirement be met gradually. Therefore, the band gap extrapolated from the small cyclic oligmers to infinite will be underestimated with a slightly steep slope. On the other hand, this deviation may be caused by the empirical extrapolation method itself, which does not express the actual asymptotic behavior.[30]

Second, both the cyclic models and the PBC calculations give the similar quinoid structure as shown in Table 4. The only difference lies in that the extent of bond alternation[17] in CYC−**PBT** (−0.088 Å) is relatively larger than that in PBC−**PBT** (−0.083 Å), which may be caused by the strain in the cyclic oligomers.

In summary, PBC and cyclic models give different descriptions of band gaps of borole-containing polymers from those extrapolated ones from the open chains through the oligomer scheme. Future experimental results are desired to test the applicability of PBC calculations to the borole-containing polymers.

4. Conclusions

The geometrical structures and electronic properties of borole/thiophene cooligomers are studied employing the hybrid density functional theory with B3LYP functional. The unrestricted DFT method gives lower ground-state energy than the spin-restricted method, indicating the radical character in borole-containing oligomers. The borole/thiophene cooligomers have the quinoid form of structures with the radical centers located at two ends of the carbon backbones. Furthermore, the biradical character is diminished slightly with the increase in the content of thiophene units. Thus, the introduction of aromatic thiophene rings can cause the stabilization effect in borole oligomers.

Band gaps of borole-containing polymers have been calculated by both the periodic boundary condition (PBC) and the cyclic oligomer model (CYC). Because of the strain and the poor coplanarity in the backbones of small cyclic oligomers, the cyclic model slightly underestimates the band gap of borole/thiophene copolymer **2** (2.00 eV) relative to the PBC band gap (2.22 eV) with the translational invariance. Both PBC and cyclic models predict the similar quinoid structure of borole/thiophene copolymer.

To summarize, the borole-containing oligomers have the quinoid structure and distinct biradical character. The introduction of thiophene rings into the oligoborole will retard the appearance of the quinoid structure and consequently stabilize the borole-containing polymers.

Acknowledgment. The authors thank two reviewers for their constructive and pertinent comments and the China NSF (Grant Nos. 90303020, 20433020, 20420150034, and 20103004) for the financial support.

Supporting Information Available: Tables of energies of oligomers n**B** ($n = {}^1/_2$−$^9/_2$), HOMO−LUMO gaps (Δ_{H-L}) and HSOMO−LSUMO gaps (Δ_{HS-LS}) of singlet and triplet systems of **1**−**3** obtained by spin restricted and unrestricted DFT method at the level of 6-31G(d). This material is available free of charge via the Internet at http://pubs.acs.org.

References and Notes

(1) Roncali, J. *Chem. Rev.* **1997**, *97*, 173−205.
(2) Kertesz, M. In *Handbook of Organic Conductive Molecules and Polymers*; Nalwa, H. S., Ed.; John Wiley & Sons Ltd.: New York, 1997; Vol. 4, pp 147−172.
(3) Bredas, J. J. *Synth. Met.* **1987**, *17*, 115.
(4) Jones, D.; Guerra, M.; Favaretto, L.; Modelli, A.; Fabrizio, M.; Distefano, G. *J. Phys. Chem.* **1990**, *94*, 5761−5766.
(5) Van Haare, J. A. E. H.; Havinga, E. E.; Van Dongen, J. L. J.; Janssen, R. A. J.; Cornil, J.; Brédas, J. L. *Chem.—Eur. J.* **1998**, *4*, 1509−1522.
(6) (a) Zhang, G.; Pei, Y.; Ma, J.; Yin, K.; Chen, C. *J. Phys. Chem. B* **2004**, *108*, 6988−6995. (b) Gao, Y.; Liu, C.; Jiang, Y. *J. Phys. Chem. A* **2002**, *106*, 5380−5384.
(7) Matsumi, N.; Miyata, M.; Chujo, Y. *Macromolecules* **1999**, *32*, 4467−4469.
(8) Yamaguchi, S.; Shirasaka, T.; Akiyama, S.; Tmao, K. *J. Am. Chem. Soc.* **2002**, *124*, 8816−8817.
(9) Douglade, G.; Febre, B. *Synth. Met.* **2002**, *129*, 309−314.
(10) Eisch, J. J.; Galle, J. E.; Kozima, S. *J. Am. Chem. Soc.* **1986**, *108*, 379−385.
(11) Salzner, U.; Lagowski, J. B.; Pickup, P. G.; Poirier, R. A. *Synth. Met.* **1998**, *96*, 177−189.
(12) Antiaromaticity of borole ring: (a) Cryañski, M. K.; Krygowski, T. M.; Katritzky, A. R.; Schleyer, P. R. *J. Org. Chem.* **2002**, *67*, 1333−1338. (b) Chesnut, D. B.; Bartolotti, L. *J. Chem. Phys.* **2000**, *253*, 1−11.
(13) De Oliveira, M. A.; Duarte, H.; Pernaut, J.; De Almeida, W. B. *J. Phys. Chem. A* **2000**, *104*, 8256−8262.
(14) Kwon, O.; Mckee, M. *J. Phys. Chem. A* **2000**, *104*, 7106−7112.
(15) Hirata, S.; Martin, H. *Chem. Phys. Lett.* **1999**, *302*, 375−382.
(16) Ma, J.; Li, S.; Jiang, Y. *Macromolecules* **2002**, *35*, 1109−1115.
(17) Zhang, G.; Ma, J.; Jiang, Y. *Macromolecules* **2003**, *36*, 2130−2140.
(18) Zhu, Z.; Wang, Y.; Lu, Y. *Macromolecules* **2003**, *36*, 9585−9593.
(19) Wang, J. F.; Feng, J. K.; Ren, A. M.; Liu, X. D.; Ma, Y. G.; Lu, P.; Zhang, H. X. *Macromolecules* **2004**, *37*, 3451−3458.
(20) Hsu, C.; Hirata, S.; Martin, H. *J. Phys. Chem. A* **2001**, *105*, 451−458.
(21) Cai, Z.; Sendt, K.; Reimers, J. R. *J. Chem. Phys.* **2002**, *117*, 5543−5549.
(22) Casida, M. E.; Jamorski, C.; Casida, K. C.; Salahub, K. R. *J. Chem. Phys.* **1998**, *108*, 4439.
(23) Tozer, D. J.; Handy, N. C. *J. Chem. Phys.* **1998**, *109*, 10180.
(24) Gaussian 03, Revision B.04. Frisch, M. J.; Trucks, G. W.; Schlegel, H. B.; Scuseria, G. E.; Robb, M. A.; Cheeseman, J. R.; Montgomery, J. A., Jr.; Vreven, T.; Kudin, K. N.; Burant, J. C.; Millam, J. M.; Iyengar, S. S.; Tomasi, J.; Barone, V.; Mennucci, B.; Cossi, M.; Scalmani, G.; Rega, N.; Petersson, G. A.; Nakatsuji, H.; Hada, M.; Ehara, M.; Toyota, K.; Fukuda, R.; Hasegawa, J.; Ishida, M.; Nakajima, T.; Honda, Y.; Kitao, O.; Nakai, H.; Klene, M.; Li, X.; Knox, J. E.; Hratchian, H. P.; Cross, J. B.; Adamo, C.; Jaramillo, J.; Gomperts, R.; Stratmann, R. E.; Yazyev, O.; Austin, A. J.; Cammi, R.; Pomelli, C.; Ochterski, J. W.; Ayala, P. Y.; Morokuma, K.; Voth, G. A.; Salvador, P.; Dannenberg, J. J.; Zakrzewski, V. G.; Dapprich, S.; Daniels, A. D.; Strain, M. C.; Farkas, O.; Malick, D. K.; Rabuck, A. D.; Raghavachari, K.; Foresman, J. B.; Ortiz, J. V.; Cui, Q.; Baboul, A. G.; Clifford, S.; Cioslowski, J.; Stefanov, B. B.; Liu, G.; Liashenko, A.; Piskorz, P.; Komaromi, I.; Martin, R. L.; Fox, D. J.; Keith, T.; Al-Laham, M. A.; Peng, C. Y.; Nanayakkara, A.; Challacombe, M.; Gill, P. M. W.; Johnson, B.; Chen, W.; Wong, M. W.; Gonzalez, C.; Pople, J. A. Gaussian, Inc., Pittsburgh, PA, 2003.
(25) Mitani, M.; Mori, H.; Takano, Y.; Yamaki, D.; Yoshilka, Y.; Yamaguchi, K. *J. Chem. Phys.* **2000**, *113*, 4035.
(26) Mitani, M.; Yamaki, D.; Takano, Y.; Kitagawa, Y.; Yoshilka, Y.; Yamaguchi, K. *J. Chem. Phys.* **2000**, *113*, 10486.
(27) Lahti, P. M.; Ichimura, A. S.; Sanborn, J. A. *J. Phys. Chem. A.* **2001**, *105*, 251.
(28) Kudin, K. N.; Scuseria, G. E. *Chem. Phys. Lett.* **1998**, *289*, 611−616.
(29) Kudin, K. N.; Scuseria, G. E. *Phys. Rev. B* **2000**, *61*, 16440−16453.
(30) Hutchison, G. R.; Zhao, Y. J.; Delley, B.; Freeman, A. J.; Ratner, M. A.; Marks, T. J. *Phys, Rev. B* **2003**, *68*, 035204.
(31) Yang, S.; Olishevski, P.; Kertesz, M. *Synth. Met.* **2004**, *141*, 171−177.

(32) Suzuki, N.; Ozaki, M.; Etemad, S.; Heeger, A. J.; MacDiarmid, A. G. *Phys. Rev. Lett.* **1980**, *45*, 1209.
(33) Lee, C.; Kang, G.; Jeon, J.; Song, W.; Kim, S.; Seoul, C. *Synth. Met.* **2001,** *117*, 75−79.
(34) Kovacic, P.; Jones, M. B. *Chem. Rev.* **1987**, *87*, 357−379.
(35) Zotti, G.; Martina, S.; Wegner, G.; Schlüter, A.-D. *Adv. Mater.* **1992**, *4*, 798−801.
(36) Kobayashi, M.; Chen, J.; Chung, T. C.; Moraes, F.; Heeger, A. J.; Wudl, F. *Synth. Met.* **1984**, *9*, 77.
(37) Chung, T, C.; Kaufmzn, J. H.; Heeger, A. J.; Wudl, F. *Phys. Rev. B.* **1984**, *30*, 702.
(38) Glenis, S.; Benz, M.; LeGoff, E.; Schindler, J. L.; Kannewurf, C. R.; Kanatzidis, M. G. *J. Am. Chem. Soc.* **1993**, *115*, 12519.
(39) Su, W. P.; Schrieffer, J, R.; Heeger, A. J. *Phys. Rev. Lett.* **1979**, *42*, 1698−1701.
(40) Shirakawa, H.; Ito, T.; Ikeda, S. *Makromol. Chem.* **1978**, *179*, 1565.
(41) Goldberg, I. B.; Crowe, H. R.; Newman, P. R.; Heeger, A. J.; MacDiarmid, A. G. *J. Chem. Phys.* **1979**, *70*, 1132.
(42) Peierls, R. E. *Quantum Theory of Solids*; **1954**, p 108.

MA048534Y